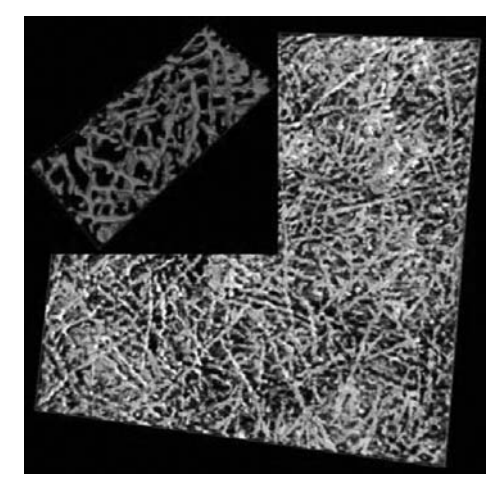


On the Importance of Morphology Control in Polymer Solar Cells

Svetlana van Bavel, Sjoerd Veenstra, Joachim Loos*

The recent progress in understanding on how the efficiency of a bulk heterojunction PSC depends on the local nanoscale volume organisation of the photoactive layer is reviewed. A quantitative analysis of the phase separation and percolation pathways was performed and

used to explain the performance of P3HT/ZnO devices with different thickness. It is concluded that the relatively poor performance of thin P3HT/ZnO solar cells is related to inefficient charge generation as a result of the low ZnO content, to the coarse phase segregation, and to the exciton losses impaired by the electrodes.



Introduction

Nanostructured polymer-based solar cells (PSCs) have emerged as a promising low-cost alternative to conventional inorganic photovoltaic devices and are now a subject of intensive research both in academia and industry. For PSCs to become practical efficient devices, several issues should still be addressed, including further understanding of their operation and stability, which in turn are largely determined by the morphological organisation in the photoactive layer. The latter is typically a few hundred nanometres thick film and is a blend composed of two materials: the bulk heterojunction consisting of the electron donor and the electron acceptor.

S. van Bavel, S. Veenstra, J. Loos

Dutch Polymer Institute, P.O. Box 902, 5600 AX Eindhoven, The Netherlands

S. van Bavel, J. Loos

Department of Chemical Engineering and Chemistry, Eindhoven University of Technology, P.O. Box 513, 5600 MB Eindhoven, The Netherlands

S Veenstra

Energy Research Centre of The Netherlands (ECN), P.O. Box 1, 1755 ZG Petten, The Netherlands

J. Loos

Department of Physics and Astronomy, University of Glasgow, Glasgow G12 8QQ, Scotland, UK

E-mail: j.loos@physics.gla.ac.uk

The main requirements for the morphology of efficient photoactive layers are nanoscale phase segregation for a high donor/acceptor interface area and hence efficient exciton dissociation, short and continuous percolation pathways of both components leading through the layer thickness to the corresponding electrodes for efficient charge transport and collection, and high crystallinity of both donor and acceptor materials for high charge mobility. In this paper, we review recent progress of our understanding on how the efficiency of a bulk heterojunction PSC largely depends on the local nanoscale volume organisation of the photoactive layer.

Solar Energy and State-of-the-Art Solar Technologies

In this century, the worldwide energy consumption is expected to grow on average with 1.5–2.0% per year.^[1] The current economic crisis (2009/10) may slow this growth down for a few years but it is unlikely to change the major picture. This trend is mostly driven by the expected growth





Svetlana van Bavel obtained her B. Sc. in chemistry (cum laude) at the Mendeleev University of Chemical Technology in Moscow, Russia in 1997. After having worked for a few years in marketing and R&D at various companies in Russia and in the Netherlands, she followed in 2003–2005 her masters studies in chemical technology at the Eindhoven University of Technology. Her graduation project on "development of a flat model catalyst for olefin polymerisation by anchoring of borane activators" was carried out in 2005 in the group of Inorganic Chemistry and Catalysis under supervision of Dr. Peter Thüne and Prof. Hans Niemantsverdriet (completed cum laude). In 2009 she received her doctorate degree (cum laude) at the same university in the group of Materials and Interface Chemistry under the mentorship of Dr. Joachim Loos and Prof. Bert de With. Her research was dedicated to studying the relationship between performance of polymer solar cells and three-dimensional nanoscale morphological organisation of their photoactive layers, and involved an intensive use of transmission electron microscopy techniques in general and electron tomography in particular. In March 2010 she joined Shell Global Solutions in Amsterdam, The Netherlands as a technologist.



Sjoerd Veenstra studied Polymer Chemistry at the University of Groningen (The Netherlands) where he graduated in 1997 after a study on organic-based bulk heterojunctions. He stayed at the same university where he received his Ph.D. degree under the supervision of Prof. G. Hadziioannou and Prof. Dr. G. A. Sawatzky, on a thesis entitled 'The Electronic Structure of Molecular Systems' in 2002. After his PhD, he accepted a position as researcher on polymer-based solar cells at the Energy Research Centre of The Netherlands (ECN). Since 2009, ECN and the Holst Centre in Eindhoven (The Netherlands) have a joint program on Organic Photovoltaics. Sjoerd Veenstra went for an internship to the University of California at Santa Barbara in the group of Prof. A. J. Heeger (1997) and as visiting scientist to the group of Prof. G. G. Malliaras at Cornell University (2005). Since 2008 he gives a course on 'Solar Cells' together with Prof. J. C. Hummelen at the University of Groningen.



Joachim Loos has received his Ph.D. in Physics from the University of Dortmund, Germany, in 1996 under supervision of Prof. Jürgen Petermann. Since 1997 he was appointed at the Department of Chemical Engineering and Chemistry of the Eindhoven University of Technology (TU/e), in the group of Prof. Piet Lemstra (later also in the group of Prof Gijsbertus de With); first as Research Fellow of the Dutch Polymer Institute (DPI), later as Assistance and Associated Professor. He has initiated and established the Soft Matter Cryo-TEM Research Unit at TU/e and was its principal investigator. He is seriously involved in the research program of the DPI and other national and international institutions. In 2010 he was appointed Professor of Solid State Physics at the Glasgow University, Scotland, UK. His research focus comprises understanding and control of organisation or assembly of polymer nanostructures, i.e., semi-conducting polymers and polymer-based conductive nanocomposites. Ultimately, the organisation of the polymer systems is tuned by applying physical principles at various length scales from (sub-) nanometre (intra- and inter-molecular organisation) up to hundreds of nanometres (e.g., phase separation and crystal superstructures) towards advanced performance of functional devices. Moreover, he develops advanced microscopy methods, mainly based on TEM, SEM and SPM.

of the overall population (6.5 billion in 2008, about 9 billion expected in 2100)^[2] and the increase in the quality of life and access to consumption for an increasing part of the world population. Most of the energy (80%) is presently derived from the combustion of fossil fuels, such as oil (35%), coal (24.5%) and natural gas (20.5%).[3] However, the world's resources of fossil fuels will 1 d be depleted: e.g., the peak of oil extraction is expected by many to occur already before 2030, followed by a terminal decline of extraction.^[4] Moreover, the use of fossil fuels releases such significant amounts of greenhouse gasses (CO₂, CH₄, N₂O) that, in case of a business-as-usual scenario, there is a high probability that the global temperature will increase with 2–5 °C in this century. In the worst case (of 5 °C), the global warming will irrevocably disturb the equilibrium of >40% of global ecosystems and endanger existence of the majority of species worldwide.[5]

Solar radiation is the renewable energy source with practically unlimited access. The amount of solar energy reaching the surface of the planet is so vast that in 1 year it is about twice as much as will ever be obtained from all of the

Earth's non-renewable resources of coal, oil, natural gas and mined uranium combined. ^[6] The total annual solar energy striking the Earth's surface is estimated to be about 7 700 times the current world annual energy consumption, and a part of it corresponding to 100 times the current world energy consumption should be realistically exploitable. ^[7]

The solar energy can be utilised in three major ways: by means of concentrated solar power (CSP) technologies aiming at collecting solar heat, concentrating it between 50 and 50 000 times and then converting it into electricity; by artificial mimicking of the photosynthesis process as happens every day in most plants on earth; and by direct conversion of sunlight into electricity in a photovoltaic (PV) process (eventually with the use of solar concentrators too). Today, large expectations are set for PVs to become a significant energy supplying technology by the end of this century. [8]

Polymer Solar Cells

In recent years, an alternative type of thin film solar cells has been intensively studied, viz. organic or polymer-based



solar cells that use organic electronic materials, such as polymer semiconductors like poly(phenylene vinylene) (PPV), polythiopene or polyfluorene, for light absorption and charge transport. [9,10] Despite comparatively low efficiencies of about 7–8%^[11] achieved so far with the modelling studies predicting 10-11% efficiencies attainable^[12] and rather low stabilities presently 1 or 2 years at maximum,[13] PSCs have a distinct advantage over inorganic counterparts, viz. their fast and low-cost manufacturing process: they can be fabricated by processing polymers, eventually together with other organic materials, in solution and depositing them by printing or coating in a roll-to-roll fashion like newspapers. Thanks to the speed and ease of this manufacturing process, the energy payback time of PSCs may, according to some estimates, be limited to months to about a year only. [8,14] Additional advantages include lightweight and flexibility of organic materials, enabling fast and easy applications on e.g., curved surfaces and thus freedom of design.

PSCs are still in the research and development phase; however, first commercial products recently were introduced to the market. To bring them closer to the stage of practical efficient devices, several issues should still be addressed, including further improvements of their efficiency and stability. These, in turn, are determined to a large extent by the morphological organisation of the photoactive layer, i.e., layer where light is absorbed and converted into electrical charges. Thus, the general scope of this paper is to look into the ways how the morphology formation of ultrathin (100–200 nm) donor/acceptor photoactive layers prepared via solvent-based techniques can be controlled and manipulated, and to establish the relationships between the (three-dimensional) morphological organisation of photoactive layers and the performance of corresponding PSCs.

Morphology Requirements of Photoactive Layers in PSCs

There is a principal difference in operation of solar cells based on inorganic semiconductors and organic (polymer) semiconductors, governed by a different magnitude of the exciton binding energy (exciton = bound electron/hole pair) in these materials. In many inorganic semiconductors, the exciton binding energy is low compared to the thermal energy at room temperature and therefore free charges are directly created under ambient conditions upon absorption of a photon of light. An organic semiconductor, on the other hand, typically possesses an exciton binding energy that exceeds kT roughly by more than an order of magnitude. As a consequence, excitons do not directly split into free charges in organic semiconductors and an additional mechanism is required to achieve this.

A successful way to dissociate excitons formed in organic semiconductors into free charges is to use a combination of two materials: an electron donor (the material with low ionisation potential) and electron acceptor (the one with large electron affinity). At the donor/acceptor interface, an exciton can dissociate into free charges by rapid electron transfer from the donor to acceptor. [17,18] Afterwards, both charge carriers move to their respective electrode when electrode materials are chosen with the proper work functions. [9] Significant PV effects of organic semiconductors applying the heterojunction approach have first been demonstrated by Tang in the 1980s (Figure 1a). [19] A thinfilm, two-layer organic PV cell has been fabricated that showed a power conversion efficiency of about 1% and a large fill factor (FF) of 0.65 under simulated AM 2 illumination.

The external quantum efficiency η_{EOE} of a PV cell based on exciton dissociation at a donor/acceptor interface is $\eta_{\rm EOE} = \eta_{\rm A} \times \eta_{\rm ED} \times \eta_{\rm CC}$, with the light absorption efficiency $\eta_{\rm A}$, the exciton dissociation efficiency $\eta_{\rm ED}$, which is the fraction of photogenerated excitons that dissociate into free charge carriers at a donor/acceptor interface, and the carrier collection efficiency η_{CC} , which is the probability that a free carrier generated at a donor/acceptor interface by dissociation of an exciton reaches its corresponding electrode. [20] Donor/acceptor interfaces can be very efficient in separating excitons: systems are known in which the forward reaction, the charge generation process takes place on the femtosecond time scale, while the reverse reaction, the charge recombination step, occurs in the microsecond range.[21] The typical exciton diffusion length in most organic semiconductors is, however, limited to 5-20 nm. [22-25] Consequently, acceptor/donor interfaces have to be within this diffusion range for efficient exciton dissociation into free charges; however, efficient light absorption only can be guaranteed for photoactive layers with thickness larger than 200 nm.

Independently, Yu and Heeger^[26] and Halls et al. ^[27] have addressed the problem of limited exciton diffusion length by intermixing two conjugated polymers with different electron affinities or a conjugated polymer with C₆₀ molecules or their methanofullerene derivatives. [28] Since phase segregation occurs between the two constituents, a large internal interface is created so that most excitons are formed near the interface and are thus able to dissociate at the interface. In case of the polymer/polymer intermixed film, evidence for the success of the approach has been found in the observation that the photoluminescence from each of the polymers was quenched. This implies that the excitons generated in one polymer within the intermixed film reach the interface with the other polymer and dissociate before decaying. This device structure, a socalled bulk heterojunction (Figure 1b), provides a route by which nearly all photogenerated excitons in the film can

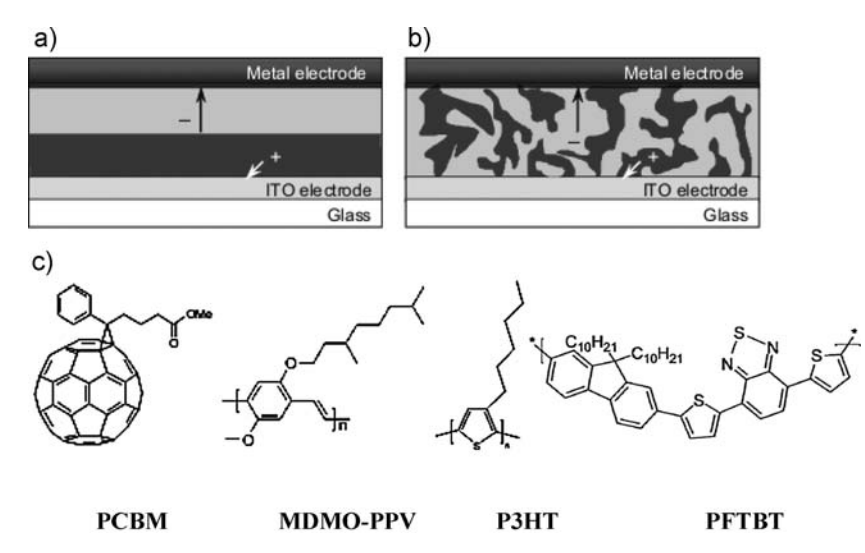


Figure 1. (a) Schematic representations of a Tang double layer cell and (b) a bulk heterojunction structure, together with (c) chemical structures of the most common electron donor and electron acceptor materials: methanofullerene derivative PCBM, MDMO-PPV, P3HT and PFTBT. The common device structure is depicted here, with a photoactive layer sandwiched between an electron collecting electrode (typically metal, such as Al) and a hole collecting transparent electrode of ITO.

split into free charge carriers. At present, bulk heterojunction structures are the main candidates for high-efficiency PSCs.

Nanoscale phase segregation between the donor and acceptor components dictated by a limited exciton diffusion length is not the only requirement for the morphology of photoactive layers of bulk heterojunction PSCs. Once free charges are formed upon exciton dissociation, they should be transported through the donor and acceptor phases towards the corresponding electrodes: holes through the donor phase to the hole collecting [positive, mainly indiumdoped tin oxide (ITO)] electrode and electrons through the acceptor phase to the electron collecting (negative, e.g., aluminium) electrode. Thus the nanoscale phases of donor and acceptor should form continuous, and preferably short (to minimise charge recombination), percolation pathways leading to the positive and negative electrodes, respectively.

Additionally, the transport of charge carriers can be enhanced if donor and/or acceptor (ideally both) are characterised by high mesoscopic order and crystal-linity. [29,30] Also, transport and collection of charges should be facilitated in case where there is enrichment of the acceptor material at the side of a photoactive layer close to a negative (metal) electrode and enrichment of the donor material close to a positive commonly used ITO electrode. [31,32] Such favourable concentration gradients of donor and acceptor materials through the thickness of the active layer should ensure that percolation pathways leading to electrodes are short and limit possibilities of charge recombination.

The efficiency of a bulk heterojunction PSC is thus largely dependent on the local nanoscale organisation of the photoactive layer in all three dimensions. The key requirements for efficient PSCs, including those dealing with photoactive layer morphology, are listed in Figure 2, together with the parameters of device performance $(J_{\rm sc}, {\rm FF}, V_{\rm oc}, \eta)$.

The short circuit current $J_{\rm sc}$ generated by a solar cell is found at the end of the whole chain: it is determined by the external quantum efficiency $\eta_{\rm EQE}$, i.e., efficiency of all basic processes of the PSC operation as discussed above, viz. light absorption, exciton dissociation at the donor/acceptor interface, and transport and collection of free charges at the electrodes. The meaning of the FF is more specific: a higher FF implies an improved balance of electron and hole transport, low traps and negligible space-charge

effects.[12,33]

The open circuit voltage V_{oc} is set by the separation of the (quasi) Fermi levels for electrons and holes. This explains why the V_{oc} scales with the energy difference between the lowest unoccupied molecular orbital (LUMO) of the acceptor material and the highest occupied molecular orbital (HOMO) of the donor. [34,35] Lower values of $V_{\rm oc}$ obtained experimentally have been attributed to the band bending created by accumulated charges at each electrode, with associated losses of ≈0.2 eV per electrode. [35,36] It has also been reported that $V_{\rm oc}$ is dependent on the probability of exciton dissociation into free charges, [37] presence of electron traps [38] and mobility of free charges. [39] As the position of the quasi Fermi levels is determined by both the shape of the densities of states (DOS) and the filling, it is straight forward that the $V_{
m oc}$ depends on the energy levels, the energetic disorder in these levels, the charge generation rate and the charge recombination rate. Since the morphology influences these four parameters, it is clear that the morphology influences the V_{oc} . However, the impact of these parameters on V_{oc} is complex and beyond the scope of this review. Comparing the J-V curves of pristine and annealed poly(3-hexylthiophene) (P3HT)/phenyl-C₆₁-butyric acid methyl ester (PCBM) samples measured under one sun gives an indication how strong the V_{oc} depends on the morphology. From ref. [30], we estimate the difference in $V_{\rm oc}$ to be around 40 mV between a pristine and annealed P3HT/PCBM sample. This is an improvement in V_{oc} of less than 10%, whereas the morphology change caused a twofold increase in the J_{sc} .



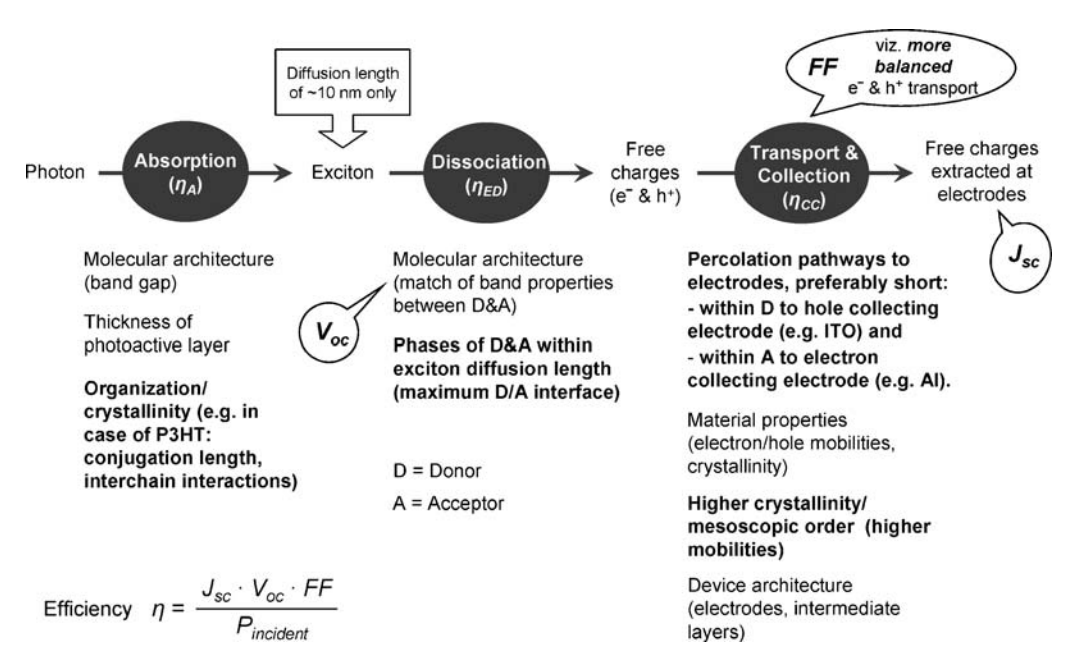


Figure 2. The key factors determining the power conversion efficiency (η) of bulk heterojunction PSCs, together with parameters of solar cell device performance: short circuit current density J_{sc} , open circuit voltage V_{oc} and FF. All three basic processes: light absorption (characterised by efficiency η_A), exciton dissociation (η_{ED}) and transport and collection of charges (η_{CC}) should be efficient in order to get efficient PSCs. The efficiency determining factors are listed under each step; those dealing with photoactive layer morphology are shown in bold.

Parameters Determining the Morphology Formation of the Photoactive Layer

The following parameters have been identified as the most significant for their influence on the nanoscale morphology in the photoactive layers of bulk heterojunction PSCs: the chemical structure of donor and acceptor materials, the solvent(s) used for processing, concentration in solution, the ratio between donor and acceptor and post-production treatments such as thermal annealing or exposure to solvent vapour. [40–42] Some examples of how these parameters affect photoactive layer morphology formation and hence device performance are considered below.

Since the photoactive layer is deposited from solution, for research studies mainly via spin-coating or drop-casting, the morphology determining parameters can be classified into two groups: due to thermodynamic aspects and kinetic effects that mainly play role during thin-film formation process. Thermodynamic aspects are reflected in the chemical structure of the donor and acceptor compounds determining to a large extent their solubility in different solvents and the interaction (miscibility) between these compounds taken in a certain ratio. The kinetic aspects have to do with duration of film formation - influenced e.g., by the solvent's boiling point, by solution viscosity, etc. –, with the rate of ordering or crystallisation in case of crystallising materials and thus accompanied reorganisation, and with post-film formation treatments such as annealing that enables the diffusion and crystallisation of one or both

compounds in the blend, leading to enhanced phase segregation.

Both thermodynamic and kinetic parameters show comparable significance in determining the morphology of the photoactive layer. Thermodynamics will, however, drive (and kinetics may limit) eventual morphological reorganisation after films have been formed, and thus determine the long-term stability of the photoactive layer morphology and corresponding solar cell devices.

Intensive morphology studies have been performed on polymer/fullerene systems, in which PCBM is applied (for its chemical structure see Figure 1c). [43,44] PCBM is by far the most widely used electron acceptor, and the most successful PSCs have been obtained by mixing it with the donor polymers like poly(2-methoxy-5-(3',7'-dimethyloctyloxy)-1,4-phenylenevinylene) (MDMO-PPV) [45,46] and other poly(phenylene vinylene) derivatives, with poly(3-alkylthiophene)s such as regioregular P3HT [30,47-50] or less studied combination with polyfluorenes [51-54] and other amorphous semi-conducting polymers such as poly{2,6-[4,4-bis-(2-ethylhexyl)-4*H*-cyclopenta[2,1-b;3,4-b']dithiophene]-alt-[4,7-(2,1,3-benzothiadiazole)]} (PCPDTBT). [55-58]

The crystallisation behaviour of PCBM when cast from solution, particularly the crystallisation kinetics induced by different solvent evaporation dynamics, has been intensively investigated.^[59–62] For all conditions it has been confirmed that crystalline PCBM domains develop. In general, the dynamics of solvent evaporation during film formation and certain post-treatment procedures play a



vital role for the crystallisation behaviour and morphology formation of PCBM from solution. For instance, PCBM has a tendency to crystallise by eventually forming micrometreslarge bulky crystals; also in mixtures with amorphous materials having rather low glass transition temperature (T_g) like MDMO-PPV $(T_g \text{ of } 80 \,^{\circ}\text{C})$.

On the contrary, the type of crystalline morphology formed by regioregular P3HT ranges from well-dispersed nanorods to well-developed spherulites, depending on solution processing conditions. [63] Typically, P3HT crystallises in thin films by forming crystalline nanorods with widths of around 15-25 nm, thickness of just a few nanometres and lengths of hundreds of nanometres or even a few micrometres. [30,42,63,64]

The influence of the solvent used for processing was first observed in MDMO-PPV/PCBM system when a strong increase in power conversion efficiency was obtained by changing the solvent from toluene (0.9% efficiency) to chlorobenzene (2.5% efficiency). [45] The better performance of MDMO-PPV/PCBM cells in case of using chlorobenzene (or o-dichlorobenzene) as a solvent rather than toluene, was found to be due to smaller (more favourable) scale of phase segregation (Figure 3), viz. smaller PCBM-rich domains in the MDMO-PPV-rich matrix, formed during spin-coating as

zene.[45,59,60,65] The evaporation rate of a solvent during film formation is

a result of higher solubility of PCBM in chloroben-

also of importance. Even when a good solvent (chlorobenzene) is taken for MDMO-PPV/PCBM but its evaporation is slowed down e.g., by using lower spin speed during spincoating or by using drop-casting instead of spin-coating, coarse phase segregation is observed in the resulting films similar to faster spin-coating from a less favourable solvent like toluene. [59] Since a film has then a longer time to form and kinetic factors become less limiting, thermodynamically driven re-organisation, viz. large-scale PCBM crystallisation, takes place. Not surprisingly, thermal annealing of MDMO-PPV/PCBM boosts PCBM crystallisation even further leading to formation of bulky PCBM crystals. Besides annealing conditions, the kinetics of their formation was also found to depend on a type of spatial confinement, e.g., in a free-standing film, PCBM clusters are formed much faster than in a film sandwiched between two substrates.[66]

Besides the solvent used and the evaporation rate applied, the overall compound concentration and the ratio between two compounds in solution are important parameters controlling morphology formation. High com-

> pound concentrations induce large-scale phase segregation in MDMO-PPV/PCBM during formation of the film. [64] The maximum solubility of PCBM was determined to be roughly 1 wt.-% in toluene and 4.2 wt.-% in chlorobenzene (at room temperature), so that for concentrations above these critical concentrations aggregation of PCBM is anticipated already in the solvent and is enhanced even further during film formation.[41]

> For the systems of MDMO-PPV/PCBM methoxy ethyl-hexyloxy-PPV/ PCBM,) as for most other amorphous polymer/PCBM bulk heterojunctions, the optimum ratio of the compounds was found to be 1:4, [28] in spite of very low contribution of PCBM to light absorption and despite the fact that photoluminescence of the polymer is already quenched for much lower PCBM concentrations (less than 5%).[18] A rather abrupt improvement in the device properties was observed for PCBM contents of around 67%, and it was accompanied by the onset of phase segregation.^[67] Thus, it was concluded that charge transportation rather than charge separation is the limiting factor here and suggested that, only above this

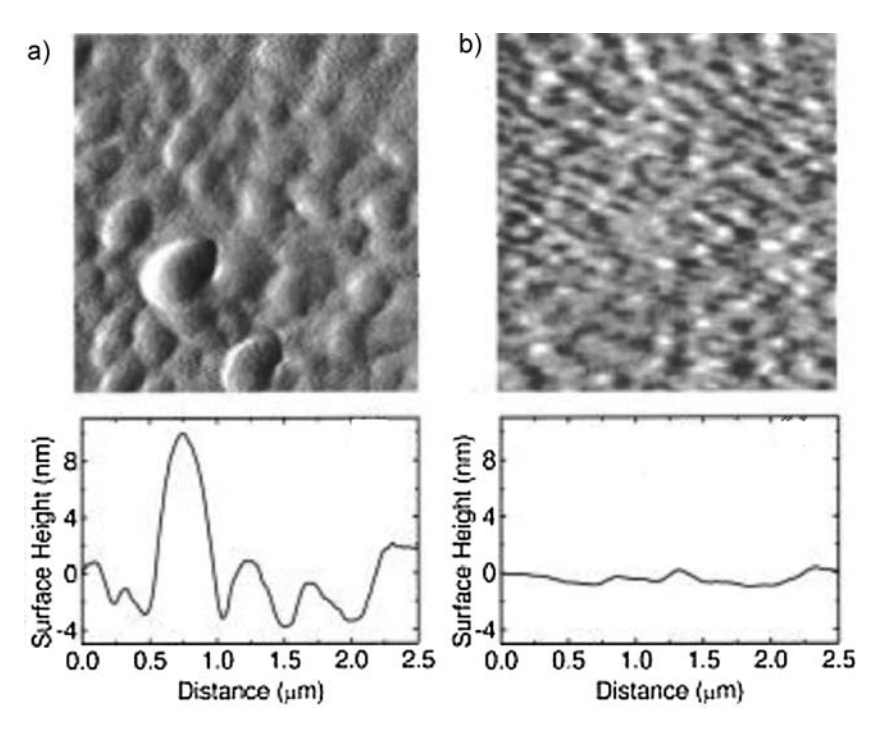


Figure 3. Atomic force microscopy images showing the surface morphology of MDMO-PPV/PCBM (1:4 w/w) blend films with a thickness of approximately 100 nm and the corresponding cross sections. (a) Film spin coated from a toluene solution. (b) Film spin coated from a chlorobenzene solution. The images show the first derivative of the actual surface heights. The cross-sections of the true surface heights for the films were taken horizontally from the points indicated by the arrow (Reprinted with permission from ref. [45] Copyright 2001 American Institute of Physics).



critical concentration, PCBM forms a percolating network within the polymer matrix.

In general, thermal annealing is a useful way to probe morphological stability of photoactive layers. Apart from accelerating thermodynamically favoured changes in the layer morphology, mild annealing also mimics practical conditions as solar cells can easily heat up during operation to temperatures of around 60 °C. Obviously, long-term stability of PSCs based on MDMO-PPV/PCBM is rather poor, due to the tendency of PCBM to crystallise by forming micrometres-large clusters in amorphous MDMO-PPV. Such large-scale crystallisation implies that exciton dissociation becomes rather inefficient, and the quality of a percolating network of PCBM deteriorates too. The formation of large PCBM crystals can, however, be largely suppressed by choosing a polymer having a higher T_g (e.g., 138 °C)^[68] than that of MDMO-PPV, so that diffusion of PCBM molecules in the blends is hindered (another example of interplay between thermodynamics and kinetics in these systems).

Another family of amorphous polymers suitable for organic PVs, are copolymers containing a fluorene unit and a benzathiadiazole unit with two neighbouring thiophene rings, often referred to as APFO3 or poly{(9,9didecanefluorene)-alt-[bis(thienylene)benzothiadiazole]} (PFTBT). [51-54,69] These copolymers have a similar band gap as P3HT, approximately 1.9 eV, but the V_{oc} is higher (1.0 V). The high voltage is explained by the fact that the HOMO of these benzathiadiazole containing polymers is about 0.5 eV further from the vacuum level. [70] When comparing the PV performance of polymer:fullerene bulk heterojunction based on either P3HT or PFTBT, the general conclusion is that the influence of the high open circuit voltage on the PV performance is compensated by comparatively low FFs and short circuit currents. [53,69] Moet et al. recently concluded that the mobility of PFTBT is sufficiently high that space charge effects on the photocurrent do not play a significant role. [71] The not-optimal device performance is attributed to a relatively low dissociation probability of short-lived bound electron-hole pairs. As discussed above, the dissociation of these excitons is to a large extend influenced by the morphology. Several attempts have been made to influence or control the morphology of blends of PFTBTs and PCBM. These attempts include different side chains, [69] solvent mixtures^[72] and ternary blends of two PFTBTs combined with PCBM. [73]. In another approach to improve the morphology of the PFTBT/PCBM blend, PFTBT analogues were synthesised with high molecular weights $(\overline{M}_{w} =$ 120 kg \cdot mol⁻¹). These blends reveal indeed phase segregation on 10-20 nm scale with two bicontinuous phases, as opposed to an even finer morphology observed for blends containing lower molecular weight PFTBT where no clear phase segregation was observed.[74]

The P3HT/PCBM system, where both components can crystallise as mentioned above, differs in its behaviour and

morphological organisation from MDMO-PPV/PCBM blends. Here the best results with power conversion efficiencies between 4 and 5% and rather stable morphologies, are obtained for P3HT/PCBM ratios of around 1:1 after an annealing treatment, either at elevated temperature or during slow solvent evaporation (so-called solvent assisted annealing). [30,50,75,76] Similar results are also attained by adding high boiling point additives like alkylthiols into the solution of P3HT/PCBM as this slows down the film formation during spin-coating due to longer solvent(s) evaporation time, analogous to solvent annealing. [56,77]

Various reasons have been named to account for morphology changes causing efficiency improvement in P3HT/PCBM films upon annealing, such as increased crystallinity of P3HT, [78] favourable dimensions of (long and thin) P3HT crystals, [63] suppressed formation of bulky PCBM clusters due to presence of P3HT crystals, [30,50] improved light absorption of the P3HT/PCBM films as a result of morphological changes in P3HT, [79] improved hole mobility and hence more balanced hole and electron transport in P3HT/PCBM films. [33,80,81] This list, however long it may seem, is not complete as it does not include details on morphological organisation throughout the volume of the photoactive layer, such as quality of percolating networks of nanocrystalline P3HT and PCBM and the exact scale of phase segregation.

In an attempted to reveal the three-dimensional organisation of the photoactive layer of P3HT/PCBM PSCs, recently the volume morphology of films were analysed in detail by means of electron tomography and the critical morphology parameters contributing to the improved performance of P3HT/PCBM solar cell devices after thermal or solvent assisted annealing were identified. [74,82,83] After annealing treatment, thermodynamically driven reorganisation of the P3HT/PCBM morphology takes place and highly crystalline and up to micrometres long P3HT nanorods compose a genuine 3D network and serve as physical barriers to PCBM diffusion suppressing a large scale phase segregation of PCBM at any time of the film preparation process (Figure 4). Moreover, accumulation of P3HT nanorods close to the bottom hole collecting electrode ensures effective hole transport with high mobility, whereas nanocrystalline PCBM, accumulated in its turn close to the top electrode, ensures efficient electron transport.

The examples just considered concerned polymer/full-erene PSCs but, in general, all the parameters influencing morphology formation are also valid for polymer/polymer systems^[84–88] and for hybrid systems, where semi-conducting polymers such as P3HT are combined with inorganic materials such as ZnO, TiO2 or CdSe.^[89–92] A potential advantage of all-polymer systems is improved absorption as compared with systems using poorly absorbing fullerenes, and hybrid solar cells form an

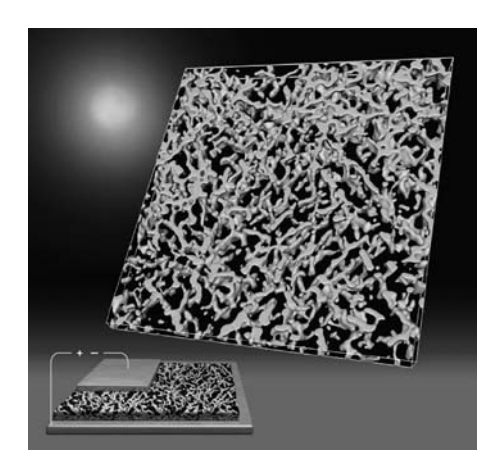


Figure 4. Volume representation obtained by electron tomography of P3HT nanorods (bright phase) in a P3HT/PCBM bulk heterojunction demonstrating the presences of a genuine 3D co-continuous network and concentration gradients within the thickness of the photoactive layer of both components. The experimental data are embedded in an artistic view on energy conversion by PSCs (Reprinted with permission from ref., [82] figure is part of the cover page. Copyright 2009 American Chemical Society).

attractive alternative because of a high dielectric constant (facilitating carrier generation processes), a high carrier mobility of inorganic semiconductors, and the thermal morphological stability of the photoactive layers.

Outlook and Challenges

As evident from the above discussion, there is a complex interplay between different aspects that determine photoactive layer morphology during film formation, its eventual re-organisation during post-production treatments and its long-term stability. Due to this complexity and due to the fact that the desired structure should form spontaneously by deposition from solution (to retain low-cost manufacturing), the optimal morphology is explored in practice by time-consuming optimisation processes. However, increasing understanding of underlying structure-property relationships should make direct manipulations possible in the future.

What complicates the matter is that the ideal photo-active layer morphology is characterised by different length-scales in the volume of the film (see Figure 1b): for efficient charge separation, it should have phases of donor and acceptor materials in the order of 5–20 nm (in two dimensions)^[22–25] and, for charge collection, it should have percolation pathways through the whole thickness of the film, i.e., a few hundred nanometres in thickness direction of the photoactive layer. The requirement of donor and acceptor phases of different length-scale in three

dimensions makes the control of spontaneous morphology formation very challenging, especially in case of thicker photoactive layers. For optimum light absorption, the layer should ideally be at least 200 nm thick, whereas it is often observed that thinner films of ca. 100–150 nm perform better in bulk heterojunction PSCs even though they effectively absorb less light. Poor performance of thicker layers is typically attributed to enhanced recombination of free charges resulting from imperfect percolation pathways.

Several attempts have been made to promote formation of such a well-organised structure through the whole volume of the photoactive layer by e.g., using an amphiphilic primary structure like diblock copolymers, $^{[93]}$ dyad structures $^{[94,95]}$ and an inorganic (ZnO_x or TiO_x) template nanostructure filled with organic semiconductors $^{[96,97]}$ but performance of the resulting solar cells has so far been lower than with conventional approaches. Moreover, creation of nanostructures already in the solvent prior to deposition might be a route to split structure formation from the film deposition process, which probably allows for better morphology control of the photoactive layer. $^{[98]}$

One key request on the way to control and optimise morphology creation is access to reliable quantitative datasets reflecting the local nanoscale as well as the overall organisation of the photoactive layer and allow for straightforward correlation of the obtained morphology with device performance. As an example, in a recent study the 3D morphology as obtained by electron tomography was statistically analysed for spherical contact distance and percolation pathways of the ZnO nanoparticles embedded in P3HT. [99] Together with solving the three-dimensional exciton diffusion equation, a consistent and quantitative correlation between solar cell performance, photophysical data and the three-dimensional morphology has been obtained for devices with different layer thickness that enables differentiating between generation and transport as limiting factors to performance (Figure 5).

Briefly, in our study the quantitative analysis of the phase separation and percolation pathways was performed and used to explain the performance of P3HT/ZnO devices with different thickness. Looking at the combined effects of charge carrier generation and collection, we concluded that the relative poor performance of thin P3HT/ZnO solar cells is related to inefficient charge generation as a result of the low ZnO content, to the coarse phase segregation, and to the exciton losses impaired by the electrodes. For thicker photoactive layers charge generation is much more efficient, owing to a much more favourable phase segregation. However, even thicker devices show superior efficiencies, still the internal quantum efficiency (IQE) only reaches 50%. Since in thicker layers most excitons (around 80%) reach the P3HT/ZnO interface where they can dissociate into free charges, the IQE is most probably



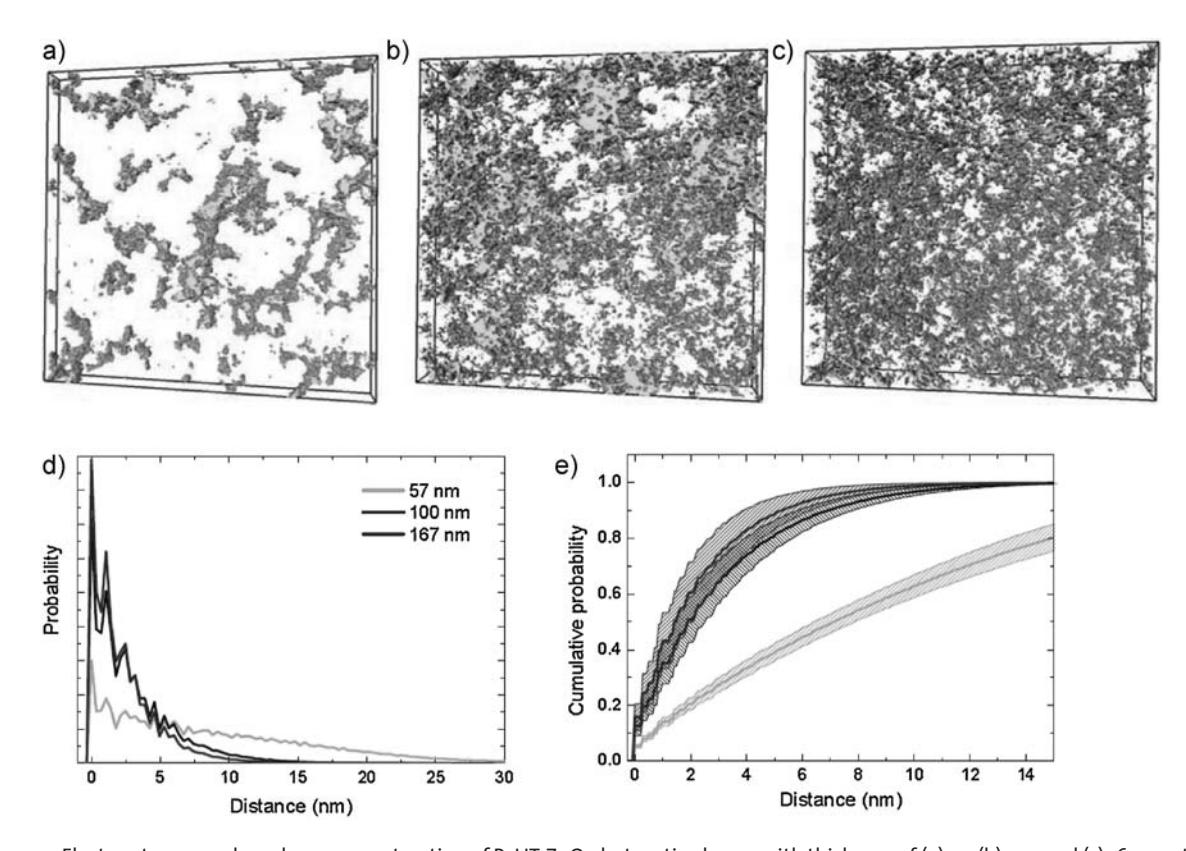


Figure 5. Electron tomography volume reconstruction of P3HT:ZnO photoactive layers with thickness of (a) 57, (b) 100 and (c) 167 nm; the size of all samples is 800×800 nm²; ZnO appears light gray, P3HT transparent. (d) Distribution of the probability to find a P3HT voxel (3D pixel) at a certain distance from a ZnO domain for mixed P3HT:ZnO films of different thickness, calculated from the 3D electron tomography data displayed in (a)–c); (e) cumulative probability to have P3HT within a shortest distance to ZnO. The error margins indicated are obtained from the two most extreme thresholds possible for the binarisation of the electron tomography volume data (Reprinted with permission from ref. [99] Copyright 2009 Nature Publishing Group).

limited by inefficient charge transport. Electron transport may be limited by a low volume fraction of ZnO, whereas hole transport may be inefficient due to low hole mobility in P3HT.

Moreover, it should be said that, besides better morphology control, device performance can also be optimised by smart device architecture, e.g., by applying hole blocking layers, [100] optical spacers to enhance light absorption in the layer of the same thickness [101,102] and by using the tandem cell architecture, [103–105] where two PV cells are added in series. In a tandem cell, it is possible to combine two, or more, thinner (more efficient) active layers and to use semiconductors with different bandgaps for more efficient light harvesting. Besides, since individual cells are added in series, the open circuit voltage of a tandem cell is directly increased to the sum of the $V_{\rm oc}$ values of individual cells.

Evidently, material properties of the donor and acceptor also have a direct impact on the performance of PSCs as they determine e.g., light absorption, mobility of free charges, and the value of the open circuit voltage (see Figure 2). A lot of efforts are now devoted to the synthesis of new materials, such as low band gap polymers [106–108] having better

overlap with the solar spectrum than the state-of-the-art polymers and alternative acceptors with a higher LUMO level than that of C_{60} or PCBM which will lead to better $V_{\rm oc}$ values in the corresponding solar-cell devices. [109–111]

Finally, modelling studies show that with optimised energy levels of the donor and acceptor (determining their absorption and $V_{\rm oc}$ of the corresponding solar cells), balanced electron and hole mobility and optimised morphology, even in case of single bulk heterojunction PSCs power conversion efficiencies of 10–11% should be within reach. [12,38]

Acknowledgements: The authors would like to use this opportunity to thank *René Janssen, Martijn Wienk, Jan Kroon, Xiaoniu Yang, Erwan Sourty* and *Gijsbertus de With* for helpful discussions and the *Dutch Polymer Institute* (DPI) for fruitful cooperation.

Received: February 4, 2010; Revised: April 22, 2010; Published online: DOI: 10.1002/marc.201000080



Keywords: bulk heterojunction; electron tomography; films; morphology; polymer solar cells

- [1] United Nations Development Program (UNDP), United Nations Department of Economy and Social Affairs (UNDESA), World Energy Council (WEC), World Energy Assessment Overview 2001, www.undp.org.
- [2] U.S. Bureau of the Census International Data Base, 2008.
- [3] International Energy Agency, Key World Energy Statistics, www.iea.org.
- [4] R. W. Bentley, Energy Policy 2002, 30, 189.
- [5] R. A. Kerr, Science 2007, 318, 1230.
- [6] W. A. Hermann, Energy 2006, 31, 1685.
- [7] N. Nakicenovic, N. A. Grubler, A. McDonald, Eds., Global Energy Perspectives, Cambridge University Press, Cambridge 1998
- [8] G. Dennler, C. Brabec, in: Organic Photovoltaics, C. Brabec, V. Dyakonov, U. Scherf, Eds., Wiley-VCH, Weinheim 2008, pp. 531–566.
- [9] S. Gunes, H. Neugebauer, N. S. Sariciftci, Chem. Rev. 2007, 107, 1324.
- [10] H. Hoppe, N. S. Sariciftci, Adv. Polym. Sci. 2008, 214, 1.
- [11] Y. Liang, Z. Xu, J. Xia, S.-T. Tsai, Y. Wu, G. Li, C. Ray, L. Yu, Adv. Mater. 2010, 22, 1.
- [12] L. J. A. Koster, V. D. Mihailetchi, P. W. M. Blom, Appl. Phys. Lett. 2006, 88, 09351.
- [13] M. Jorgensen, K. Norrman, F. C. Krebs, Sol. Energy Mater. Sol. Cells 2008, 92, 686.
- [14] A. L. Roes, E. A. Alsema, K. Blok, M. K. Patel, Prog. Photovolt. : Res. Appl. 2009, 17, 372.
- [15] R. H. Bube, *Photoelectronic Properties of Semiconductors*, Cambridge University Press, Cambridge 1992.
- [16] M. Pope, C. E. Swenberg, Electronic Processes in Organic Crystals and Polymers, Oxford University Press, Oxford 1999.
- [17] N. S. Sariciftci, L. Smilowitz, A. J. Heeger, F. Wudl, *Science* 1992, *I*, 1474.
- [18] A. Haugeneder, M. Neges, C. Kallinger, W. Spirkl, U. Lemmer, J. Feldmann, U. Scherf, E. Harth, A. Gügel, K. Müllen, Phys. Rev. B 1999, 59, 15346.
- [19] C. W. Tang, Appl. Phys. Lett. 1986, 48, 183.
- [20] P. Peumans, A. Yakimov, S. R. Forrest, J. Appl. Phys. 2003, 93,
- [21] L. Smilowitz, N. S. Sariciftci, R. Wu, C. Gettinger, A. J. Heeger, F. Wudl, *Phys. Rev. B* **1993**, *47*, 13835.
- [22] K. Yoshino, Y. X. Hong, K. Muro, S. Kiyomatsu, S. Morita, A. A. Zakhidov, T. Noguchi, T. Ohnishi, Jpn. J. Appl. Phys. 2 1993. 32. L357.
- [23] J. J. M. Halls, K. Pichler, R. H. Friend, S. C. Moratti, A. B. Holmes, Appl. Phys. Lett. 1996, 68, 3120.
- [24] T. J. Savenije, J. M. Warman, A. Goossens, Chem. Phys. Lett. 1998, 287, 148.
- [25] J. E. Kroeze, T. J. Savenije, M. J. W. Vermeulen, J. M. Warman, J. Phys. Chem. B 2003, 107, 7696.
- [26] G. Yu, A. J. Heeger, J. Appl. Phys. 1995, 78, 4510.
- [27] J. J. M. Halls, C. A. Walsh, N. C. Greenham, E. A. Marseglia, R. H. Friend, S. C. Moratti, A. B. Holmes, *Nature* **1995**, *376*, 498.
- [28] G. Yu, J. Gao, J. C. Hummelen, F. Wudl, A. J. Heeger, Science 1995, 270, 1789.
- [29] H. Sirringhaus, P. J. Brown, R. H. Friend, M. M. Nielsen, K. Bechgaard, B. M. W. Langeveld-Voss, A. J. H. Spiering, R. A. J. Janssen, E. W. Meijer, P. Herwig, D. M. de Leeuw, *Nature* 1999, 401, 685.

- [30] X. Yang, J. Loos, S. C. Veenstra, W. J. H. Verhees, M. M. Wienk, J. M. Kroon, M. A. J. Michels, R. A. J. Janssen, *Nano Lett.* 2005, 5, 579.
- [31] Y. Kim, S. A. Choulis, J. Nelson, D. D. C. Bradley, S. Cook, J. R. Durrant, Appl. Phys. Lett. 2005, 86, 063502.
- [32] S. Heutz, P. Sullivan, B. M. Sanderson, S. M. Schultes, T. S. Jones, Sol. Energy Mater. Sol. Cells 2004, 83, 229.
- [33] V. D. Mihailetchi, H. X. Xie, B. de Boer, L. J. A. Koster, P. W. M. Blom, Adv. Funct. Mater. 2006, 16, 699.
- [34] V. D. Mihailetchi, P. W. M. Blom, J. C. Hummelen, M. T. Rispens, J. Appl. Phys. 2003, 94, 6849.
- [35] C. J. Brabec, A. Cravino, D. Meissner, N. S. Sariciftci, T. Fromherz, M. T. Rispens, L. Sanchez, J. C. Hummelen, Adv. Funct. Mater. 2001, 11, 374.
- [36] M. C. Scharber, D. Mühlbacher, M. Koppe, P. Denk, C. Waldauf, A. J. Heeger, C. J. Brabec, Adv. Mater. 2006, 18, 789.
- [37] L. J. A. Koster, V. D. Mihailetchi, R. Ramaker, P. W. M. Blom, Appl. Phys. Lett. **2005**, 86, 123509. The expression in question has the following form: $V_{\rm oc} = E_{\rm gap}/q (kT/q) * \ln [C^*(1-P)/P]$, where P is the dissociation probability of excitons into free charges. Unless P is approaching zero, the dependency of $V_{\rm oc}$ on P can be neglected.
- [38] M. M. Mandoc, F. B. Kooistra, J. C. Hummelen, B. de Boer, P. W. M. Blom, Appl. Phys. Lett. 2007, 91, 263505.
- [39] M. M. Mandoc, L. J. A. Koster, P. W. M. Blom, *Appl. Phys. Lett.* **2007**, *90*, 133504. Very high carrier mobilities (above 10^{-3} m $^2 \cdot V^{-1} \cdot s^{-1}$) affect the difference between the quasi-Fermi levels and lead to the reduction of $V_{\rm oc}$. For comparison, mobilities of holes and electrons in annealed P3HT/PCBM blends are around 10^{-8} and 10^{-7} m $^2 \cdot V^{-1} \cdot s^{-1}$, respectively [34].
- [40] H. Hoppe, N. S. Sariciftci, J. Mater. Chem. 2006, 16, 45.
- [41] X. Yang, J. Loos, Macromolecules 2007, 40, 1353.
- [42] B. C. Thompson, J. M. J. Fréchet, Angew. Chem., Int. Ed. 2008, 47, 58.
- [43] J. C. Hummelen, B. W. Knight, F. LePeq, F. Wudl, J. Gao, C. L. Wilkins, J. Org. Chem. 1995, 60, 532.
- [44] F. Wudl, Acc. Chem. Res. 1992, 25, 157.
- [45] S. E. Shaheen, C. J. Brabec, N. S. Sariciftci, F. Padinger, T. Fromherz, J. C. Hummelen, Appl. Phys. Lett. 2001, 78, 841.
- [46] A. Mozer, P. Denk, M. Scharber, H. Neugebauer, N. S. Sariciftci, P. Wagner, L. Lutsen, D. Vanderzande, J. Phys. Chem. B 2004, 108, 5235.
- [47] F. Padinger, R. S. Rittberger, N. S. Sariciftci, *Adv. Funct. Mater.* **2003**. *13*. 85.
- [48] C. Waldauf, P. Schilinsky, J. Hauch, C. J. Brabec, Thin Solid Films 2004, 451, 503.
- [49] M. Al-Ibrahim, O. Ambacher, S. Sensfuss, G. Gobsch, Appl. Phys. Lett. 2005, 86, 201120.
- [50] W. Ma, C. Yang, X. Gong, K. Lee, A. J. Heeger, Adv. Funct. Mater. 2005, 15, 1617.
- [51] M. Svensson, F. Zhang, S. C. Veenstra, W. J. H. Verhees, J. C. Hummelen, J. M. Kroon, O. Inganäs, M. R. Andersson, Adv. Mater. 2003, 15, 988.
- [52] T. Yohannes, F. Zhang, M. Svensson, J. C. Hummelen, M. R. Andersson, O. Inganäs, *Thin Solid Films* 2004, 449, 152.
- [53] L. H. Slooff, S. C. Veenstra, J. M. Kroon, D. J. D. Moet, J. Sweelssen, M. M. Koetse, Appl. Phys. Lett. 2007, 90, 143506.
- [54] O. Inganäs, F. Zhang, M. R. Andersson, Acc. Chem. Res. 2009, 42, 1731.
- [55] R. Kroon, M. Lenes, J. C. Hummelen, P. W. M. Blom, B. de Boer, Polym. Rev. 2008, 48, 531.
- [56] J. Peet, J. Y. Kim, N. E. Coates, W. L. Ma, D. Moses, A. J. Heeger, G. C. Bazan, Nat. Mater. 2007, 6, 497.



- [57] R. Qin, W. Li, C. Li, C. Du, C. Veit, H.-F. Schleiermacher, M. Andersson, Z. Bo, Z. Liu, O. Inganäs, U. Würfel, F. Zhang, J. Am. Chem. Soc. 2009, 131, 14612.
- [58] T.-Y. Chu, S. Alem, P. G. Verly, S. Wakim, J. Lu, Y. Tao, S. Beaupré, M. Leclerc, F. Bélanger, D. Désilets, S. Rodman, D. Waller, R. Gaudiana, Appl. Phys. Lett. 2009, 95, 063304.
- [59] X. Yang, J. K. J. van Duren, R. A. J. Janssen, M. A. J. Michels, J. Loos, *Macromolecules* 2004, 37, 2152.
- [60] H. Hoppe, M. Niggemann, C. Winder, J. Kraut, R. Hiesgen, A. Hinsch, D. Meissner, N. S. Sariciftci, Adv. Funct. Mater. 2004, 14, 1005.
- [61] X. Yang, J. K. J. Van Duren, M. T. Rispens, J. C. Hummelen, R. A. J. Janssen, M. A. J. Michels, J. Loos, Adv. Mater. 2004, 16, 802.
- [62] H. Yang, T. J. Shin, L. Yang, K. Cho, C. Y. Ryu, Z. Bao, Adv. Funct. Mater. 2005, 15, 671.
- [63] K. J. Ihn, J. Moulton, P. Smith, J. Polym. Sci., Part B: Polym. Phys. 1993, 31, 735.
- [64] J. A. Merlo, C. D. Frisbie, J. Phys. Chem. B 2004, 108, 19169.
- [65] M. T. Rispens, A. Meetsma, R. Rittberger, C. J. Brabec, N. S. Sariciftci, J. C. Hummelen, Chem. Commun. 2003, 2116.
- [66] X. Yang, A. Alexeev, M. A. J. Michels, J. Loos, *Macromolecules* 2005, 38, 4289.
- [67] J. K. J. van Duren, X. Yang, J. Loos, C. W. T. Bulle-Lieuwma, A. B. Sieval, J. C. Hummelen, R. A. J. Janssen, Adv. Funct. Mater. 2004, 14, 425.
- [68] S. Bertho, G. Janssen, T. J. Cleij, B. Conings, W. Moons, A. Gadisa, J. D'Haen, E. Goovaerts, L. Lutsen, J. Manca, D. Vanderzande, Sol. Energy Mater. Sol. Cells 2008, 92, 753
- [69] M.-H. Chen, J. Hou, Z. Hong, G. Yang, S. Sista, L.-M. Chen, Y. Yang, Adv. Mater. 2009, 21, 4238.
- [70] D. Veldman, S. C. J. Meskers, R. A. J. Janssen, Adv. Funct. Mater. 2009, 19, 1939.
- [71] D. J. D. Moet, M. Lenes, J. D. Kotlarski, S. C. Veenstra, J. Sweelssen, M. M. Koetse, B. de Boer, P. W. M. Blom, Org. Electron. 2009, 10, 1275.
- [72] F. Zhang, K. G. Jespersen, C. Björström, M. Svensson, M. R. Andersson, V. Sundström, K. Magnusson, E. Moons, A. Yartsev, O. Inganäs, Adv. Funct. Mater. 2006, 16, 667.
- [73] A. Gadisa, F. Zhang, D. Sharma, M. Svensson, M. R. Andersson, O. Inganäs, *Thin Solid Films* 2007, 515, 3126.
- [74] S. S. van Bavel, E. Sourty, G. de With, S. Veenstra, J. Loos, J. Mater. Chem. 2009, 19, 5388.
- [75] G. Li, V. Shrotriya, J. Huang, Y. Yao, T. Moriarty, K. Emery, Y. Yang, Nat. Mater. 2005, 4, 864.
- [76] M. Reyes-Reyes, K. Kim, D. Carroll, Appl. Phys. Lett. 2005, 87, 083506.
- [77] J. Peet, C. Soci, R. C. Coffin, T. Q. Nguyen, A. Mikhailovsky, D. Moses, G. C. Bazan, Appl. Phys. Lett. 2006, 89, 252105.
- [78] Y. Zhao, G. X. Yuan, P. Roche, M. Leclerc, Polymer 1995, 36, 2211.
- [79] D. Chirvase, J. Parisi, J. C. Hummelen, V. Dyakonov, Nanotechnology 2004, 15, 1317.
- [80] T. J. Savenije, J. E. Kroeze, X. Yang, J. Loos, Adv. Funct. Mater. 2005, 15, 1260.
- [81] L. J. A. Koster, V. D. Mihailetchi, M. Lenes, P. W. M. Blom, in: Organic Photovoltaics, C. Brabec, V. Dyakonov, U. Scherf, Eds., WILEY-VCH, Weinheim 2008, pp. 283–298.
- [82] S. S. van Bavel, E. Sourty, G. de With, J. Loos, *Nano Lett.* 2009, 9, 507.
- [83] S. S. van Bavel, E. Sourty, G. de With, K. Frolic, J. Loos, Macromolecules 2009, 42, 7396.

- [84] P. A. van Hal, M. P. T. Christiaans, M. M. Wienk, J. M. Kroon, R. A. J. Janssen, J. Phys. Chem. B 1999, 103, 4352.
- [85] J. J. M. Halls, A. C. Arias, J. D. MacKenzie, W. Wu, M. Inbasekaran, W. P. Woo, R. H. Friend, Adv. Mater. 2000, 12, 498.
- [86] U. Stalmach, B. de Boer, C. Videlot, P. F. van Hutten, G. Hadziioannou, J. Am. Chem. Soc. 2000, 122, 5464.
- [87] F. Zhang, M. Jonforsen, D. M. Johansson, M. R. Andersson, O. Inganäs, Synth. Met. 2003, 138, 555.
- [88] S. C. Veenstra, W. J. H. Verhees, J. M. Kroon, M. M. Koetse, J. Sweelssen, J. J. A. M. Bastiaansen, H. F. M. Schoo, X. Yang, A. Alexeev, J. Loos, U. S. Schubert, M. M. Wienk, *Chem. Mater.* 2004, 16, 2503.
- [89] B. R. Saunders, M. L. Turner, Adv. Colloid Interface Sci. 2008, 138. 1.
- [90] W. J. E. Beek, M. M. Wienk, R. A. J. Janssen, Adv. Mater. 2004, 16, 1009.
- [91] W. U. Huynh, J. J. Dittmer, A. P. Alivisatos, Science 2002, 295, 2425.
- [92] C. Y. Kuo, W. C. Tang, C. Gau, T. F. Guo, D. Z. Jeng, Appl. Phys. Lett. 2008, 93, 033307.
- [93] S. Jenekhe, X. L. Chen, Science 1998, 279, 1903.
- [94] T. Nishizawa, H. K. Lim, K. Tajima, K. Hashimoto, Chem. Commun. 2009, 2469.
- [95] C. Yang, J. K. Lee, A. J. Heeger, F. Wudl, J. Mater. Chem. 2009, 19, 5416.
- [96] D. C. Olson, J. Piris, R. T. Collins, S. E. Shaheen, D. S. Ginley, Thin Solid Films 2006, 496, 26.
- [97] K. Coakley, M. D. McGehee, Appl. Phys. Lett. 2003, 83, 3380
- [98] A. J. Moule, K. Meerholz, Adv. Funct. Mater. 2009, 19, 3028.
- [99] S. D. Oosterhout, M. M. Wienk, S. S. van Bavel, R. Thiedmann, L. J. A. Koster, J. Gilot, J. Loos, V. Schmidt, R. A. J. Janssen, *Nat. Mater.* 2009, 8, 818.
- [100] A. Hayakawa, O. Yoshikawa, T. Fujieda, K. Uehara, S. Yoshikawa, Appl. Phys. Lett. 2007, 90, 163517.
- [101] H. Hansel, H. Zettl, G. Krausch, R. Kissilev, M. Thelakkat, H.-W. Schmidt, Adv. Mater. 2003, 15, 2056.
- [102] J. Gilot, I. Barbu, M. M. Wienk, R. A. J. Janssen, Appl. Phys. Lett. 2007. 91. 113520.
- [103] J. Y. Kim, K. Lee, N. E. Coates, D. Moses, T.-Q. Nguyen, M. Dante, A. J. Heeger, Science 2007, 317, 222.
- [104] J. Gilot, M. M. Wienk, R. A. J. Janssen, Appl. Phys. Lett. 2007, 90. 143512.
- [105] A. Hadipour, B. de Boer, J. Wildeman, F. B. Kooistra, J. C. Hummelen, M. Turbiez, M. M. Wienk, R. A. J. Janssen, P. W. M. Blom, Adv. Funct. Mater. 2006, 16, 1897.
- [106] M. M. Wienk, M. G. R. Turbiez, J. Gilot, R. A. J. Janssen, Adv. Mater. 2008, 20, 2556.
- [107] M. Heeney, W. Zhang, D. J. Crouch, M. L. Chabinyc, S. Gordeyev, R. Hamilton, S. J. Higgins, I. McCulloch, P. J. Skabara, D. Sparrowe, S. Tierney, *Chem. Commun.* 2007, 47, 5061.
- [108] A. P. Zoombelt, M. Fonrodona, M. M. Wienk, A. B. Sieval, J. C. Hummelen, R. A. J. Janssen, *Org. Lett.* 2009, 11, 903.
- [109] C. R. McNeill, A. Abrusci, J. Zaumseil, R. Wilson, M. J. McKiernan, J. H. Burroughes, J. J. M. Halls, N. C. Greenham, R. H. Friend, Appl. Phys. Lett. 2007, 90, 193506.
- [110] F. B. Kooistra, J. Knol, F. Kastenberg, L. M. Popescu, W. J. H. Verhees, J. M. Kroon, J. C. Hummelen, Org. Lett. 2007, 9, 551.
- [111] M. Lenes, G.-J. A. H. Wetzelaer, F. B. Kooistra, S. C. Veenstra, J. C. Hummelen, P. W. M. Blom, Adv. Mater. 2008, 20, 2116.

